Fabrication, characterization and effects of CuO nanoparticles on the optical behavior of polypyrrole polymeric films

H. A. Al-Yousef[a], B. M. Alotaibi[a], A. Atta[b], E. Abdeltwab[b,*],
M. M. Abdel-Hamid[c]
[a]Department of Physics, College of Science, Princess Nourah bint Abdulrahman University, P.O. Box 84428, Riyadh 11671, Saudi Arabia
[b]Physics Department, College of Science, Jouf University, P.O. Box: 2014, Sakaka, Saudi Arabia
[c]Charged Particles Lab., Radiation Physics Department, National Center for Radiation Research and Technology (NCRRT), Egyptian Atomic Energy Authority (EAEA), Cairo, Egypt

The successful preparation of flexible PPy/CuO nanocomposite consisting of polypyrrole (PPy) with copper oxide (CuO) was achieved. The structural analysis of PPy and PPy/CuO was conducted by EDX, SEM, TEM, and FTIR techniques, which providing the successful fabrications of PPy/CuO nanocomposite films. The EDX analysis of thePPy/CuO nanocomposite reveals the presence of characteristic peaks corresponding to the elements of C, Cu, N, and O, with weight percentages of 47.46%, 9.05%, 19.08%, and 24.41%, respectively. The obtained results provide confirmation that the PPy/CuO nanocomposite film does not exhibit the presence of any impurity components. The FTIR noticed that all peaks of PPy spectrum also showed in the spectra of PPy/CuO nanocomposite films with a little shifts in peaks, in which these shifts increase with increasing contents of CuO nanoparticles. The findings of this study indicate that there are interactions occurring between PPy/CuO. Furthermore, SEM was employed to elucidate the morphological of the (PPy) and PPy/CuO. The SEM demonstrate that the copper oxide (CuO) are evenly distributed within the nanocomposite films. Using Tauc's relation, the band gap and Urbach energy of PPy and PPy/CuO films. were determined. The addition of varying concentrations (2.5%, 5%, and 10%) of CuO to PPy increase the Urbach tail of PPy, resulting in energy values of 1.08 eV, 1.11 eV, and 1.13 eV, correspondingly. Simultaneously, the presence of CuO causes reduction in the band gap of PPy from 3.42 eV to 3.35 eV, 3.32 eV, and 3.30 eV. Consequently, the incorporation of CuO into PPy/CuO composite films induces both structural and optical modifications, rendering these films suitable for utilization in optoelectronic devices.

1. Introduction

Polymer nanocomposites provide a multitude of features that render them highly appealing suitable for numerous uses [1,2]. Integrating nanoparticles into a polymer matrix results in the reinforcement of the material, which improvements its mechanical properties such as stiffness, and toughness [3, 4]. Therefore, the incorporation of nanoparticles into composite materials leads to enhanced impact resistance, fracture toughness, and fatigue resistance. Consequently, nanocomposites exhibit favorable characteristics for structural applications that necessitate exceptional strength and long-lasting performance [5,6]. The increased mechanical, thermal, electrical, and surface properties of polymer nanocomposites contribute to their diverse range of features and applications [7, 8]. These technologies are utilized in several industries such as automotive, aerospace, electronics, and textiles[9].

Polymers exist in diverse manifestations, encompassing plastics, rubber, and fibers, and they exhibit a broad spectrum of utility across industries like packaging, automotive, textiles, and electronics. Polymeric films have the potential to serve as selective optical filters because of their adjustable absorption characteristics [10]. The selective transmission or blocking of specific wavelengths can be achieved in PPy films through the management of doping level or polymer structure. This characteristic makes PPy films suitable for various applications as optical telecommunications [11]. PPy has the capability to be deposited as thin films on a range of substrates, thereby imparting optical devices with desirable attributes such as flexibility and lightweight properties. The characteristics hold significant importance in the wearable technology, flexible displays, and optoelectronic devices that necessitate both conformability and portability [12]. Polypyrrole exhibits favorable biocompatibility, thereby enabling its seamless incorporation into many devices, including bioelectronics, biosensors, and implantable optoelectronic devices [13, 14]. PPy demonstrates notable stability when exposed to environmental variables such as moisture and oxygen, hence augmenting its longevity in optical systems. The maintenance of stability is of utmost importance in ensuring sustained performance and dependability over an extended period of time.

Nanoparticle fillers are characterized by their minute size, often falling within the range of 1-100 nanometers [15]. The nanoparticles under consideration possess the potential to exhibit metallic, ceramic, or organic characteristics [16]. Polymer nanocomposites are formed by incorporating nanoparticle fillers into polymers, resulting in the combination of distinctive characteristics from both the polymer matrix and the nanoparticles [17, 18].

Copper oxide nanocomposites have garnered significant attention in the optoelectronics sector due to their distinct properties and possible uses [19, 20]. Copper oxide nanocomposites demonstrate superior optical characteristics. The integration of nano-scale particles or structures has the potential to enhance the optical properties of materials, including their ability to absorb, emit, and scatter light. The manipulation of the size, shape, and content of the nanomaterials integrated into the composite enables the modulation of the optical bandgap of copper oxide nanocomposites [21, 22]. The ability to adjust the properties of materials enables the creation of materials that possess specific absorption or emission characteristics, rendering them well-suited for use in optoelectronic devices such as photodetectors and sensors [23]. Copper oxide nanocomposites exhibit a notable level of conductivity, rendering them well-suited for optoelectronic applications that necessitate effective charge transportation, such as transparent conductive electrodes employed in displays and solar cells [24].

The primary focus of the present study revolves around the manufacture of polypyrrole (PPy) encapsulated nano-CuO. This approach has demonstrated significant efficacy in the development of cost-effective and high-performing electrochemical materials. The composite material was subjected to analysis utilizing FTIR, EDX, SEM and TEM. Furthermore, an examination of the optical characteristics of the composites was conducted. The results obtained in this study demonstrate that the Ppy/CuO nanocomposites have favorable physiochemical properties that make them acceptable for applied in photovoltaics and optoelectronics.

2. Experimental work

All chemicals including pyrrole (Py monomer), HCl, and $CuSO_4$ were purchased by Sigma-Aldrich and. In which, The PPy is fabricated using the in-situ polymerization technique, which was reported in [25, 26]. Firstly, for fabrication a PPy film on glass, the pyrrole monomer (90 mmol) commbined by 0.08 M HCl in the ice bath. Subsequently, 80 mL of the ammonium persulfate (0.6 M) has been prepared as pre-cooled aqueous [27]. Then, both solutions have been blended, and continues stirred. This process made a polymerization of PPy and creation a dark green film on glass. For preparation the PPy/CuO nanocomposite films on glass, during the polymerization reaction, different ratios 20, 40, and 60 mmol of $CuSO_4$ has been incorporated with the Py monomer. As a result of this procedure, PPy/CuO films of various quantities of CuO were produced, which have been labeled as PPy/CuO-1, PPy/CuO-2, and PPy/CuO-3 films, respectively.

Furthermore, FTIR is used to show the function groups of samples (Shimadzu FTIR-340) in the 3900-400 cm^{-1} range, which provides insight into the structures of the generated PPy and PPy/CuO films. EDX (JSM-5600 JEOL, Japan) is used to determine the composite's constituent elements. The morphological were analyzed by FE-SEM (Hitachi ,S-4800). The films are prepared for scanning and measuring by having a small layer of gold sputtered onto them. At 30 mA for 30 seconds, sputtering takes place. At 200 kV, the JEOL JEM-2100 TEM transmission electron microscope achieves its maximum resolution. The optical analysis in the region of 200-1050 nm is verified using a Perkin Elmer Lamba 950 (USA) spectrophotometer.

3. Results and discussion

The element mapping and energy-dispersive X-ray (EDX) were applied to characterize and qualitative elements components of PPy/CuO-3 composite film. Figure 1(a) shows the element mapping of C, Cu, N, and O, in which these elements were distributed in the composite and confirms the existence of CuO and PPy. Figure 1(b) reveals the EDX of the PPy/CuO-3, which presents peaks of C, Cu, N, and O with weight percentages of 47.46, 9.05, 19.08, 24.41%. These findings demonstrate the absence of impurities in the PPy/CuO hybrid material [28, 29].
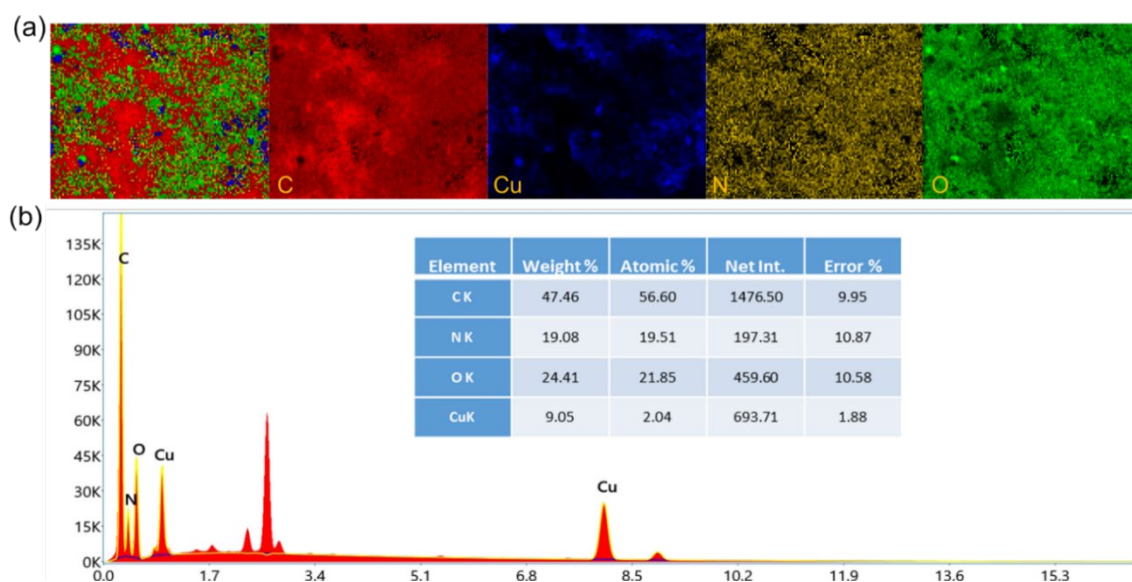

Element	Weight %	Atomic %	Net Int.	Error %
C K	47.46	56.60	1476.50	9.95
N K	19.08	19.51	197.31	10.87
O K	24.41	21.85	459.60	10.58
Cu K	9.05	2.04	693.71	1.88

Fig. 1. (a) Mapping and (b) EDX analyzes of PPy/CuO-3 nanocomposite film.

By FT-IR vibrational spectra, also the chemical interactions of PPy and CuO NPs were investigated. Figure 2 records the FTIR of of PPy and PPy/CuO with different concentrations of CuO. The spectrum of the pristine PPy presents number of characteristic bands, e.g.; 1537 cm^{-1} (stretching of C=C), 1457 cm^{-1} (C–N stretching), 1300 cm^{-1} (vibration of C-H), 1147 cm^{-1} (stretching of C–C), and 1028 cm^{-1} (N-H in-plane vibration modes) [30]. Moreover, this spectrum also holds peaks at ~ 852, 794, and 663 cm^{-1} are appeared due to the C–H bending vibrations, C–C out of plane ring deformation and C–H rocking peaks, respectively. These peaks verify the production of conductive PPy through the polymerization of PPy. [31]. Small band also was observed in spectrum of PPy at ~ 2991 cm^{-1} corresponds to the (N–H and C–H) aromatic stretching. For nanocomposite films, one can be noticed that all peaks of PPy spectrum also showed in the PPy/CuO spectra with little shifts in peaks, in which these shifts increase with increasing contents of CuO nanoparticles. This result suggests the developed interactions between various materials that presented in the nanocomposites. In addition, introducing of CuO nanoparticles also led to decreasing the intensity of bands that means the increasing of the free electrons in nanocomposite samples to be more convenient for optoelectronic characteristics, in

154

nanocomposite materials. [32]. Above all this, it is interesting to note appearing peak at ~ 550 cm^{-1} in PPy /CuO-3 which indicate to the Cu–O vibrations bond [33].
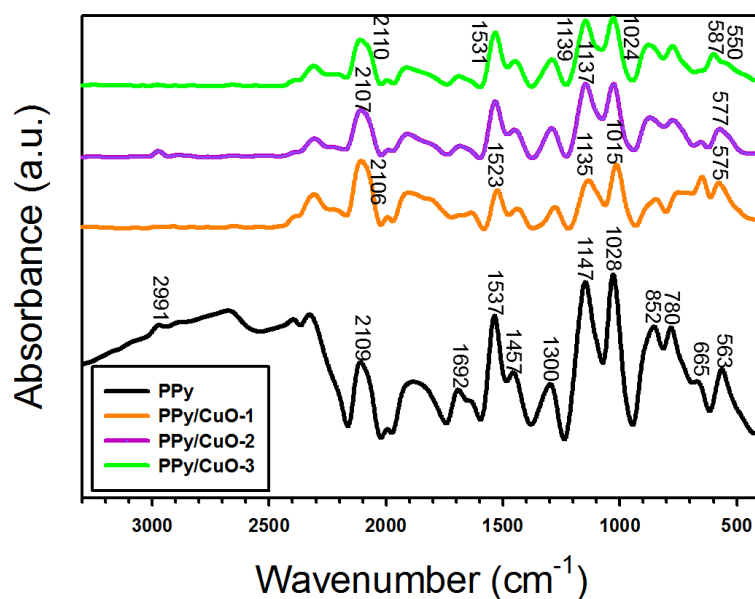

Fig. 2. FTIR of the PPy and PPy/CuO films.

The properties of morphological and distribution of various contents in the PPy and PPy/CuO films have been analyzed utilizing the SEM technique as displayed in Figure 3(a, b), accordingly. The particles of PPy acquire a cauliflower-like morphology of almost spherical nature with some agglomerations as recorded in Figure 3(a), which agree well many studies [32]. Further, the image of PPy/CuO-3 film in Figure 3(b) also shows the same morphology of the pristine PPy, but with large grains. The same morphology of PPy/CuO-3 film is associated with the filler CuO intercalation with PPy matrix [33].
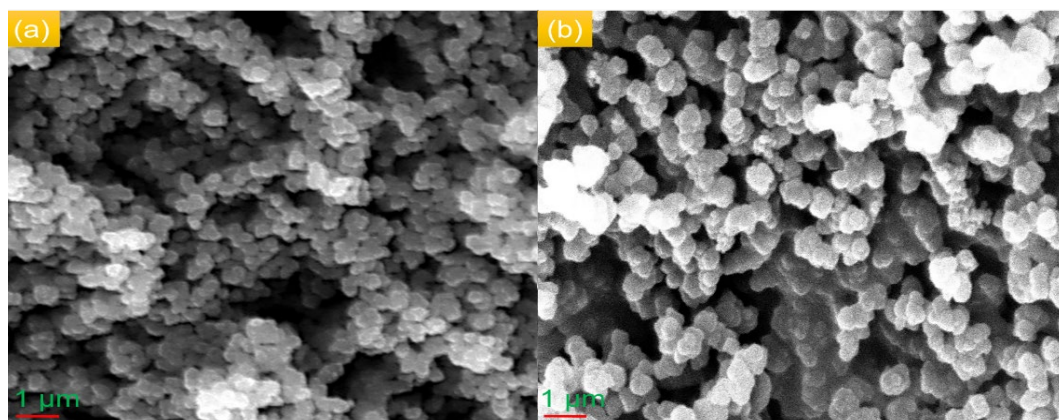

Fig. 3. SEM images of (a) the PPy. (b) PPy/CuO-3 nanocomposite film.

For further characterization, the TEM images of the PPy/CuO-3 nanocomposite film were depicted in Figure 4(a, b) under different magnifications. One can be seen that a semispherical particles of CuO (darkcolor) were formed with different sizes between 250 nm to 400 nm as shown in Figure 4(a). Further, Figure 4(b) shows that CuO particles were formed upper the surface of polypyrrole (grey color) and also between its particles. The SAED pattern of the PPy/CuO-3

nanocomposite film was included with Figure 4(b). The patterns with presence of some bright spots confirmed that the PPy /CuO nanocomposite film is crystalline in nature [34, 35]
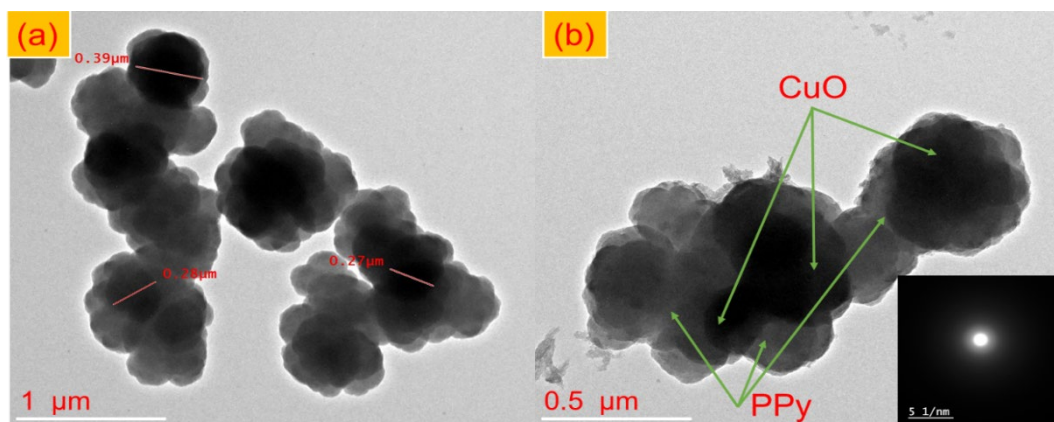

Fig. 4. (a, b) TEM images with 2 magnifications of PPy/CuO-3 nanocomposite.

Figure 5 displays the absorbance spectrum of both pure PPy and PPy/CuO films of varying CuO ratios. Absorbance behavior is consistent across each sample, this is a result of CuO's intrinsic band gap absorbance. The intensity of the absorption peaks rose from low to high as the CuO concentration was raised from 2.5 to 10%, as illustrated in Fig. 5. The reason for this is due to CuO NPs can affect the formation of complex coordination links involving CuO and PPy links [37,38]. Figure 5 further shows that all of the films exhibit a characteristic absorption band, which may be traced back to electronic transitions. The volume of the bands is increased when CuO is mixed with PPy. A higher absorption value can be achieved by incorporating CuO into the PPy. This result showed that the PPy chains are compatible with CuO. The incorporation of CuO nanoparticles into PPy was found to be an efficient method of regulating its spectral characteristics.
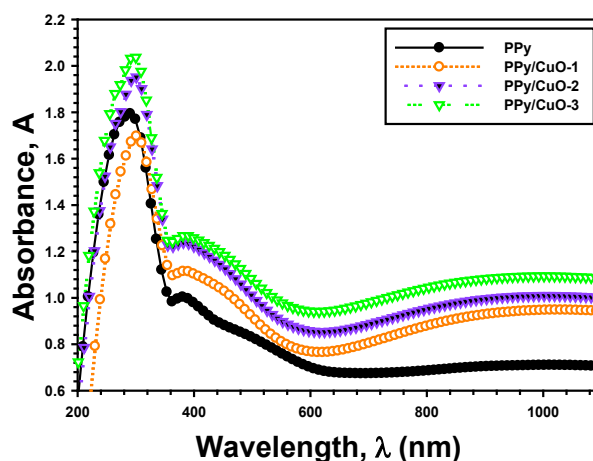

Fig. 5. Absorbance intensity versus wavelength λ, for PPy and PPy/CuO.

Applying the Beer-Lambert [39] approach, the coefficient of absorption (α) is computed by:

$$\alpha = \frac{2.303\ A}{d} \tag{1}$$

A is the optical absorbance and d is the thickness. Figure 6 displays the optical absorption coefficients (α) of pure PPy and PPy/CuO with of incident photon energy (hv). When more CuO is added, the PPy has higher absorbance coefficients. The induction of level changes by CuO adding is a possible explanation for this change [40]. Figure 4b shows how extending the linear components against hv leads to zero absorption, which may be used to determine the absorption edge E_e values for PPy and PPy/CuO films. After incorporating 2.5%, 5%, and 10% CuO, the PPy absorbs at a lower energy level (3.01, 2.96, and 2.89 eV, correspondingly) than it does (3.14 eV). The CuO nanofiller can be employed to precisely adjust the optical band gap of PPy, as seen by the red shift in the absorption edge of the PPy/CuO composites. The redshift of the absorption edge in the samples was used to infer the bonding between the CuO nanofiller and PPy. Doping the PPy with metal oxide (CuO) has been measured to have a discernible effect on the absorption coefficient. Once CuO was included, the absorption coefficient values for the proposed composites changed toward the smaller energy range.
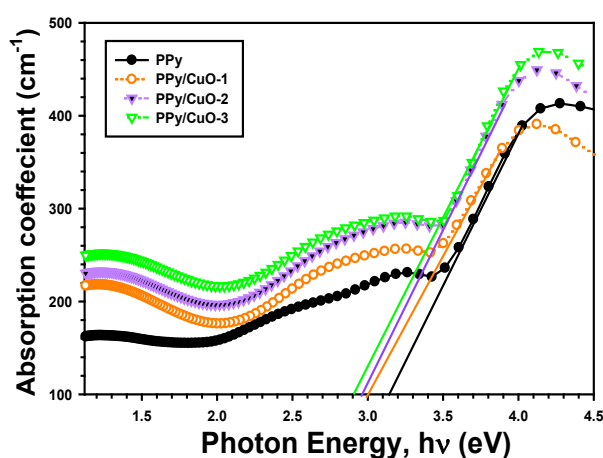

Fig. 6. Absorbance coefficient with photon energy, for PPy and PPy/CuO.

For PPy and PPy/CuO, the optical bandgap Eg is calculated using Tauc's formula. by [40].

$$\alpha h\nu = A \, (h\nu - E_g)^m \tag{2}$$

The energy gap, E_g, is the product of the photon's kinetic energy, hv, and the constant absorption rate, A. To determine the band gap, we extrapolate the straight lines from the charts depicting the correlation between $(h\nu)^2$ and incident photon energy $h\nu$ given in Figure 7. The band gap energy for PPy decreases from 3.42 eV to 3.35 eV when mixed with 2.5% CuO, 3.32 eV when combined with 5% CuO, and 3.3 eV when combined with 10% CuO. The produced CuO charge carrier causes the band gap to narrow. The high miscibility between CuO and PPy chains is demonstrated by this reduction. These findings also indicated that composites are increasingly suitable for use in optoelectronic devices. What's more, the charge-transfer complexes (CTCs) are responsible for the reduction in the optical gap. Taha et al. [40] provide evidence for this kind of behavior, the band gap narrowed with increasing NiONPs content, leading to states within the PVC optical band gap. From the optical gap Eg, we may calculate the carbon number (N) using the formula $E\_g = 34.4/N$ [41]. Table 1 displays the PPy and PPy/CuO N values. Increasing the CuO from 2.5% to 5% and 10% raises the N value for PPy from 102 to 105, 107, and 109, respectively. The narrowing of the band gap and the strengthening of N have led to this increase in CuO concentration.. Matrices–nanofiller bonds occur from matrix crystallinity variations, which affect film band gap. Variations in matrix crystalline structure cause polymer–nanofiller bindings. Visual inspection additionally altered the shade from pure PPy to semitransparent. This shows that the specimens that were made absorbed a lot of light across the spectrum. Therefore, nanocomposite films may be excellent UV absorber.
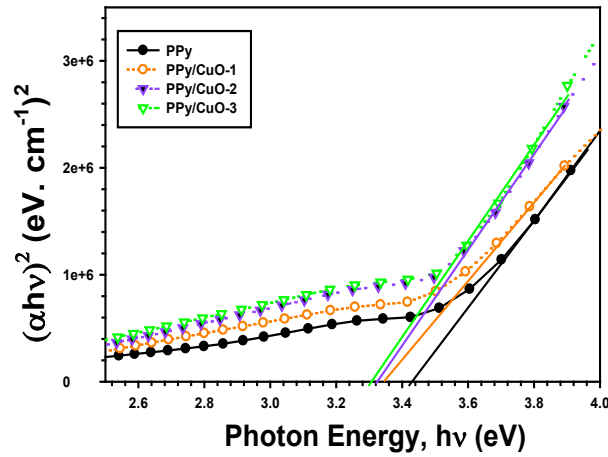
Fig. 7. The band gap as a function of the incident photon energies, for PPy and PPy/CuO.

Urbach's energy, indicating the tails portion or widened band modes in weak-photon energy spectrum, is given by [41]:

$$\alpha(\nu) = \alpha_o \, e^{h\nu/E_u} \qquad (3)$$

where α_0 is a constant and E_u is the band tail. Figure 8 shows the result of the band tail of PPy and PPy/CuO as a measure of photon energy. Band tails of PPy and PPy/CuO samples are estimated using the inverse slope of the linear parts, as shown in Table 2. It's worth mentioning that when pure PPy is coupled with 2.5%, 5%, and 10% CuO, the estimated Urbach tail of the PPy increases from 0.93 eV to 1.08 eV, 1.11 eV, and 1.13 eV, correspondingly. Increases in disorder explain why Urbach tail values go up as CuO concentration goes up. Urbach energies increase with increasing graphene oxides due to variation in the nanocomposite disorder, hence this performance is analogous to that of graphene oxide (fGO) incorporated into PVC [42].
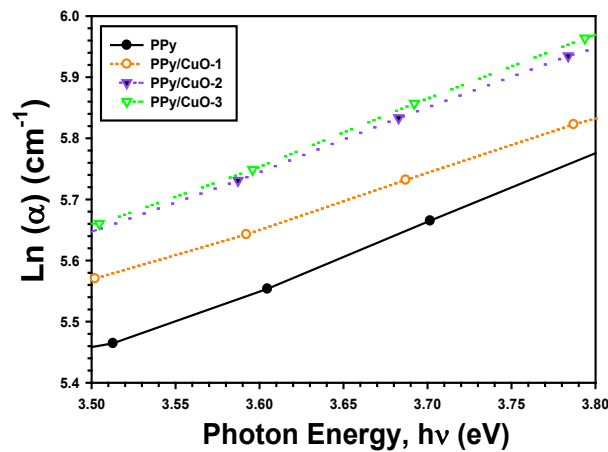

Fig. 8. Logarithm of absorption coefficient, as a function of the incident photon energies, for PPy and PPy/CuO.

158

Table 1. E_e, E_u and E_g values of PPy and PPy/CuO.

# Sample	E_e (eV)	E_g (eV)	E_u (eV)	Carbon cluster number (N)
Ppy	3.14	3.42	0.93	102
PPy/CuO-1	3.01	3.35	1.08	105
PPy/CuO-2	2.96	3.32	1.11	107
PPy/CuO-3	2.89	3.30	1.13	109

4. Conclusion

The flexible polymer nanocomposite of PPy /CuO were successfully prepared by the cast method. EDX, TEM and FTIR confirm the successful fabrication of PPy /CuO films. The EDX depicts the element mapping of C, Cu, N, and O, in which these elements were distributed in the omposite and confirms the existence of CuO and PPy. Moreover, SEM images also showed the effect of the morphological surface of the PPy after incorporation the Cuo. The crystallite size of Cu and CuO in the nanocomposite PPy /CuO-1 is 35.75 nm and 17.9 nm, respectively, which decreased in the PPy/CuO-3 nanocomposite to be 31.62 and 13.58 nm. The optical characteristics of the PPy and PPy /CuO were estimated. The CuO is induced homopolar links that causes reduction in band gap of the PPy /CuO composite. These homopolar connections cause defects to occur, which narrows the energy gap by creating a constrained state. Adding 2.5%, 5%, and 10% CuO decreases the band gap energy of PPy from 3.42 eV to 3.35, 3.32, and 3.30 eV. This decreasing of band gap is attributed to the CuO charge carrier. The above findings show that the PPy /CuO sheets have enhanced linear and non-linear optical features, making them more suitable for usage in devices involving optics.

Acknowledgment

References

[1] Alotaibi, B. M., Al-Yousef, H. A., Alsaif, N. A., Atta, A. (2022), Surface Innovations, 40, 1-13; https://doi.org/10.1680/jsuin.22.00026

[2] Atta, A., Abdelhamied, M. M., Essam, D., Shaban, M., Alshammari, A. H., Rabia, M. (2022). International Journal of Energy Research, 46(5), 6702-6710; https://doi.org/10.1002/er.7608

[3] Ahmad, W., Ahmad, Q., Yaseen, M., Ahmad, I., Hussain, F., Mohamed Jan, B., Kenanakis, G. (2021), Nanomaterials, 11(9), 2372; https://doi.org/10.3390/nano11092372

[4] Agobi, A. U., Ekpunobi, A. J., Ikeuba, A. I., Louis, H. (2022), Results in Optics, 8, 100261; https://doi.org/10.1016/j.rio.2022.100261

[5] Camargo, P.H.C., Satyanarayana, K.G., Wypych, F., 2009, Mater. Res. 12 (1), 1-39; https://doi.org/10.1590/S1516-14392009000100002

[6] Liu, Z., Liu, Q., Huang, Y.i., Ma, Y., Yin, S., Zhang, X., Sun, W., Chen, Y., 2008, Adv. Mater. 20 (20), 3924-3930; https://doi.org/10.1002/adma.200800366

[7] Mohamed, A. M., Alamri, H. R., & Hamad, M. A. (2022), Russian Journal of Physical Chemistry A, 96(10), 2259-2264; https://doi.org/10.1134/S0036024422100235

[8] Iqubal, S. M. (2022), Journal of Umm Al-Qura University for Applied Sciences, 1-4; https://doi.org/10.1007/s43994-022-00007-4

[9] Ashour G., Hussein M., Sobahi T., (2021), Journal of Umm Al-Qura University for Applied Science 7 (1), (2021) 1-6.

[10] Alotaibi, B. M., Al-Yousef, H. A., Alsaif, N. A., Atta, A. (2022), Inorganic Chemistry Communications, 144, 109904; https://doi.org/10.1016/j.inoche.2022.109904

[11] Althubiti, N. A., Abdelhamied, M. M., Abdelreheem, A. M., Atta, A. (2022), Inorganic Chemistry Communications, 137, 109229; https://doi.org/10.1016/j.inoche.2022.109229

[12] Krishnaswamy, S.; Ragupathi, V.; Raman, S.; Panigrahi, P.; Nagarajan, G.S., Optik 2019, 194, 163034; https://doi.org/10.1016/j.ijleo.2019.163034

[13] Kamal, S., Khan, F., Kausar, H., Khan, M.S., Ahmad, A., Ishraque Ahmad, S., Asim, M., Alshitari, W., Nami, S.A.A., 2020, Polym. Compos. 41 (9), 3758-3767; https://doi.org/10.1002/pc.25673

[14] Radhakrishnan, A., Rejani, P., Beena, B. (2015), Main Group Metal Chemistry, 38(5-6), 133-143; https://doi.org/10.1515/mgmc-2015-0017

[15] Radhakrishnan, A., Rejani, P., & Beena, B. (2015), Main Group Metal Chemistry, 38(5-6), 133-143; https://doi.org/10.1515/mgmc-2015-0017

[16] Moarref, P., Pishvaei, M., Soleimani-Gorgani, A., Najafi, F. (2016), Designed Monomers and Polymers, 19(2), 138-144; https://doi.org/10.1080/15685551.2015.1124321

[17] Malook, K., Khan, M., Ali, M. (2019), Journal of Materials Science: Materials in Electronics, 30, 3882-3888l; https://doi.org/10.1007/s10854-019-00673-x

[18] Abdelhamied, M. M., Atta, A., Abdelreheem, A. M., Farag, A. T. M., El Okr, M. M. (2020), Journal of Materials Science: Materials in Electronics, 31, 22629-22641; https://doi.org/10.1007/s10854-020-04774-w

[19] Farooq, A., Saleem, M.H., Ahmed, B.J., 2020, Eurasia J Biosci 14, 2969-2974.

[20] Ma, Y.u., Zhao, D., Chen, Y., Huang, J., Zhang, Z., Zhang, X., Zhang, B., 2019, Chem. Pap. 73 (1), 119-129; https://doi.org/10.1007/s11696-018-0556-x

[21] Radhakrishnan, A.; Rejani, P.; Beena, B., Int. J. Nano Dimen. 2014, 5, 519-524.

[22] Bouazizi, N.; Bargougui, R.; Oueslati, A.; Benslama, R., Adv. Mater. Lett. 2015, 6, 158-164; https://doi.org/10.5185/amlett.2015.5656

[23] Majumdar, D.; Ghosh, S., J. Energy Storage 2020, 34, 101995; https://doi.org/10.1016/j.est.2020.101995

[24] Abdelhamied, M. M., Atta, A., Abdelreheem, A. M., Farag, A. T. M., El Sherbiny, M. A. (2021), Inorganic Chemistry Communications, 133, 108926; https://doi.org/10.1016/j.inoche.2021.108926

[25] Allen, R., Pan, L., Fuller, G. G., & Bao, Z. (2014), ACS applied materials & interfaces, 6(13), 9966-9974; https://doi.org/10.1021/am5019995

[26] Atta, A., Abdeltwab, E., Negm, H., Al-Harbi, N., Rabia, M., Abdelhamied, M. M. (2023), Journal of Inorganic and Organometallic Polymers and Materials, 1-13; https://doi.org/10.1007/s10904-023-02643-7

[27] Kandulna, R., Choudhary, R. B., Kachhap, B., Kumar, A. (2023), Optik, 171393; https://doi.org/10.1016/j.ijleo.2023.171393

[28] Sadeghi, M., Shabani-Nooshabadi, M., Ansarinejad, H. (2023), Environmental Research, 216, 114633; https://doi.org/10.1016/j.envres.2022.114633

[29] Helli, M., Sadrnezhaad, S. K., Hosseini-Hosseinabad, S. M., Vahdatkhah, P. (2023), Journal of Applied Electrochemistry, 1-11; https://doi.org/10.1007/s10800-023-01955-3

[30] Majumder, M., Choudhary, R. B., Thakur, A. K., & Karbhal, I. (2017), RSC advances, 7(32), 20037-20048; https://doi.org/10.1039/C7RA01438D

[31] Sowmiya, G., & Velraj, G. (2020), Journal of Inorganic and Organometallic Polymers and Materials, 30, 5217-5223; https://doi.org/10.1007/s10904-020-01656-w

[32] Abdelhamied, M. M., Atta, A., Abdelreheem, A. M., Farag, A. T. M., El Okr, M. M. (2020), Journal of Materials Science: Materials in Electronics, 31, 22629-22641; https://doi.org/10.1007/s10854-020-04774-w

[33] Pendashteh, A., Mousavi, M. F., Rahmanifar, M. S. (2013), Electrochimica Acta, 88, 347-357; https://doi.org/10.1016/j.electacta.2012.10.088

[34] Huang, C., Tang, J., Liu, Y., Chen, T., Qi, J., Sun, S., Wu, M. (2023), Acta Biomaterialia; https://doi.org/10.1016/j.actbio.2023.06.002

[35] Debiemme-Chouvy, C. (2009), Electrochemistry communications, 11(2), 298-301; https://doi.org/10.1016/j.elecom.2008.11.030

[36] Huyen, D. N., Tung, N. T., Vinh, T. D., Thien, N. D. (2012), Sensors, 12(6), 7965-7974; https://doi.org/10.3390/s120607965

[37] Dey, S., Kar, A. K. (2019), Materials Today: Proceedings, 18, 1072-1076; https://doi.org/10.1016/j.matpr.2019.06.566

[38] Biju, R., JR, V. R., Ravikumar, R., Indulal, C. R. (2022), Plant Nano Biology, 2, 100016; https://doi.org/10.1016/j.plana.2022.100016

[39] Rao CVS, Ravi M, Raja V, Bhargav PB, Sharma AK, Rao VN (2012), Iranian Polymer Journal, 21(8): 531-536; https://doi.org/10.1007/s13726-012-0058-6

[40] Taha T, Hendawy N, El-Rabaie S, Esmat A, El-Mansy M (2019), Polymer Bulletin, 76: 4769-4784; https://doi.org/10.1007/s00289-018-2633-2

[41] Zaki MF, Ali AM and Amin RM (2017), Journal of Adhesion Science and Technology, 31(12): 1314-1327; https://doi.org/10.1080/01694243.2016.1255455

[42] Taha, T. A., Saleh, A. (2018), Applied Physics A, 124(9), 600; https://doi.org/10.1007/s00339-018-2026-2